Acta Mechanica 184, 87–101 (2006)
DOI 10.1007/s00707-005-0302-7

Acta Mechanica
Printed in Austria

Series solutions of unsteady boundary layer flow of a micropolar fluid near the forward stagnation point of a plane surface

H. Xu, **S. J. Liao**, Shanghai, China, and **I. Pop**, Cluj, Romania

Received August 16, 2005; revised October 17, 2005
Published online: April 10, 2006

Summary. In this paper, the unsteady boundary-layer flow of a micropolar fluid started impulsively from rest near the forward stagnation point of a two-dimensional plane surface is studied by means of an analytic approach, namely homotopy analysis method. This approach gives accurate approximations uniformly valid for all dimensionless time. Besides, analytic results are given for the reduced velocity and microrotation profiles, as well as for the skin friction coefficient when the material parameter K takes the value $K=0$ (Newtonian fluid), 1, 3, 5 and 10. To the best of our knowledge, such a kind of series solutions has been never reported.

1 Introduction

Stagnation point flows are classic problems in the field of fluid dynamics and have been investigated by many researchers. These flows can be viscous or inviscid, steady or unsteady, two-dimensional or three-dimensional, normal or oblique, and forward or reverse. Hiemenz [1] and Homann [2] initiated the study of two-dimensional and axisymmetric three-dimensional stagnation point flows, respectively. Wang [3] made an analysis on radial steady stagnation point flows that impinged axisymmetrically on a circular cylinder. Gorla [4] investigated the boundary-layer flow of a micropolar fluid near an axisymmetric stagnation point on a cylinder. Proudman and Johnson [5], and Robins and Howarth [6] studied the unsteady boundary layer flow near a two-dimensional rear stagnation point of a cylinder which started impulsively with a constant velocity normal to the surface of the plane. Howarth [7], [8] extended the work of Proudman and Johnson [5] and Robins and Howarth [6] on boundary-layer growth at a two-dimensional rear stagnation point to the axisymmetric (e.g., the rear of a sphere) and three-dimensional rear stagnation points. Further, Katagiri [9] considered the unsteady flow at the forward stagnation point in the presence of a uniform magnetic field. Burdé [10] investigated the effects of blowing through a porous flat surface on the unsteady stagnation point flow. Lok et al. [11] solved the unsteady boundary-layer flow of a micropolar fluid which was started impulsively with a constant velocity from rest near the forward stagnation point of an infinite plane wall.

It is worth mentioning that studies of micropolar fluids have recently received considerable attention due to their application in a number of processes that occur in industry. Such

applications include the extrusion of polymer fluids, solidification of liquid crystals, cooling of a metallic plate in a bath, animal bloods, exotic lubricants and colloidal and suspension solutions, for example, for which the classical Navier-Stokes theory is inadequate.

The essence of the theory of micropolar fluid flow lies in the extension of the constitutive equations for Newtonian fluids so that more complex fluids can be described by this theory. In this theory, rigid particles contained in a small fluid volume element are limited to rotation about the center of the volume element described by the micro-rotation vector. Physically micropolar fluids may be described as the non-Newtonian fluids consisting of dumb-bell molecules or short rigid cylindrical elements, polymer fluids, fluid suspensions, animal blood, etc. The presence of dust or smoke, particularly in a gas, may also be modelled using micropolar fluid dynamics. The theory of micropolar fluids, first proposed by Eringen [12], [13] is capable of describing such fluids. The key points to note in the development of Eringens microcontinuum mechanics are the introduction of new kinematic variables, e.g., the gyration tensor and microinertia moment tensor, and the addition of the concept of body moments, stress moments, and microstress averages to classical continuum mechanics. However, a serious difficulty is encountered when this theory is applied to real, nontrivial flow problems; even for the linear theory, a problem dealing with simple microfluids must be formulated in terms of a system of nineteen partial differential equations in nineteen unknowns, and the underlying mathematical problem is not easily amenable to solution. These special features for micropolar fluids were discussed in a comprehensive review paper of the subject and application of micropolar fluid mechanics by Ariman et al. [14], and in the recent books by Lukaszewicz [15] and Eringen [16].

The aim of the present paper is to study the unsteady boundary-layer flow of a micropolar fluid, which is started impulsively toward the wall from rest near the forward stagnation point of an infinite plane wall and to obtain the series solutions of this problem. To the best of our knowledge, no one has reported such kind of series solutions which are valid for all time $0 \leq \tau < \infty$ in the whole region $0 \leq \eta < \infty$. Recently, Liao [17] proposed a new analytic method for highly nonlinear problems, namely the homotopy analysis method (HAM). Different from perturbation techniques [18], the homotopy analysis method does not depend upon any small or large parameters and thus is valid for many nonlinear problems in science and engineering. Besides, it logically contains other non-perturbation techniques such as Lyapunov's small parameter method [19], the δ-expansion method [20], and Adomian's decomposition method [21]. The homotopy analysis method has been successfully applied to many nonlinear problems [22]–[25].

2 Mathematical description

Consider the unsteady boundary-layer flow of a micropolar fluid near the forward stagnation point of an infinite plane wall. As shown in Fig. 1a, the fluid, which occupies a semi-infinite domain bounded by an infinite plane and remains in rest for time $t < 0$, starts to move impulsively toward the wall at $t = 0$. Cartesian coordinates (x, y) fixed in space are taken, the x-axis being along the wall and the y-axis normal to it, respectively. It is well known that the boundary-layer equations governing the unsteady flow of a viscous micropolar fluid with constant properties are, see Rees and Bassom [27],

$$\frac{\partial u}{\partial x} + \frac{\partial v}{\partial y} = 0, \tag{1}$$

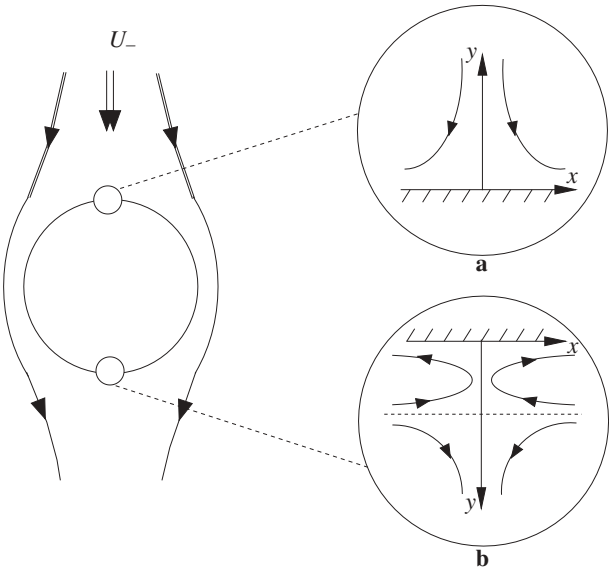

Fig. 1. Unsteady flow of a micropolar fluid in the regions of stagnation points: **a** forward stagnation point; **b** rear stagnation point (see [26])

$$\frac{\partial u}{\partial t}+u\frac{\partial u}{\partial x}+v\frac{\partial u}{\partial y}=u_e\frac{du_e}{dx}+\left(\frac{\mu+\kappa}{\rho}\right)\frac{\partial^2 u}{\partial y^2}+\frac{\kappa}{\rho}\frac{\partial N}{\partial y}, \tag{2}$$

$$\rho j\left(\frac{\partial N}{\partial t}+u\frac{\partial N}{\partial x}+v\frac{\partial N}{\partial y}\right)=\gamma\frac{\partial^2 N}{\partial y^2}-\kappa\left(2N+\frac{\partial u}{\partial y}\right), \tag{3}$$

subject to the initial/boundary conditions

$$t<0: u(t,x,y)=0,\quad v(t,x,y)=0,\quad N(t,x,y)=0, \tag{4.1}$$

$$t=0: u(t,x,\infty)=u_e(t,x),\quad N(t,x,\infty)=0, \tag{4.2}$$

$$t>0: u=0,\quad v=0,\quad N=-n\frac{\partial u}{\partial y}\ \text{at}\ y=0, \tag{4.3}$$

$$u\to u_e(x),\quad N\to 0\ \text{as}\ y\to\infty, \tag{4.4}$$

where u and v are the velocity components along x- and y-axes, N is the component of the micro-rotation vector normal to the x-y plane, ρ is the density, μ is the absolute viscosity, κ is the vortex viscosity, γ is the spin-gradient viscosity given by $\gamma=(\mu+\kappa/2)j$ (see [28]), j is the micro-inertia density, $n\in[0,1]$ is a constant, and $u_e(x)$ is the free stream velocity defined by $u_e(x)=ax$ with $a(>0)$ being a constant of dimension t^{-1}. We follow the work of many authors by assuming that j is a constant, and therefore it will be set equal to a reference value, say $j_0=\nu/a$. It should be mentioned that the boundary-layer equations (1)–(3) are valid for large values of the Reynolds number Re ($\gg 1$), where $Re=U_\infty L/\nu$ with U_∞ being the constant free stream velocity, L is a characteristic length and ν is the kinematic viscosity of the fluid. Thus the constant a can be defined as $a=U_\infty/L$ (for more details, refer to [26]).

Note that the case $n=0$, which indicates $N=0$, represents concentrated particle flows in which the microelements close to the wall surface are unable to rotate (Jena and Mathur [30]). This case is also known as the strong concentration of microelements (see Guram and Smith [31]). The case $n=1/2$ indicates the vanishing of the anti-symmetric part of the stress tensor and denotes weak concentration [32] of microelements. The case $n=1$, as suggested by Ped-

dieson [33], is used for the modelling of turbulent boundary layer flows. We shall consider here both the cases $n = 0$ and $n = 1/2$, respectively. However, it is easily shown that for $n = 1/2$ the governing equations can be reduced to the classical problem of unsteady boundary layer flow of a viscous and incompressible fluid (Newtonian fluid) near the forward stagnation point of a plane wall.

Let ψ denote the stream function. Following Nazar et al. [29] and Lok et al. [11], we use the new similarity transformations

$$\psi = \sqrt{av}x\xi f(\eta,\xi), \quad N = \sqrt{\frac{a^3}{v}}\frac{x}{\xi}g(\eta,\xi), \quad \eta = \sqrt{\frac{a}{v}}\frac{y}{\xi}, \quad \xi = \sqrt{1-\exp(-4\tau)}, \quad \tau = at. \tag{5}$$

Thus, Eqs. (2) and (3) become

$$(1+K)f_{\eta\eta\eta} + (1-\xi^2)\left[2\eta f_{\eta\eta} - 2\xi f_{\eta\xi}\right] + Kg_\eta + \xi^2\left[1 + ff_{\eta\eta} - f_\eta^2\right] = 0, \tag{6}$$

$$\left(1+\frac{K}{2}\right)g_{\eta\eta} + (1-\xi^2)\left[2g + 2\eta g_\eta - 2\xi g_\xi\right] + \xi^2\left[fg_\eta - gf_\eta - K\left(2g + f_{\eta\eta}\right)\right] = 0, \tag{7}$$

subject to the boundary conditions

$$f(0,\xi) = f_\eta(0,\xi) = 0, \quad g(0,\xi) = -nf_{\eta\eta}(0,\xi), \quad f_\eta(\infty,\xi) = 1, \quad g(\infty,\xi) = 0, \tag{8}$$

where $K = \kappa/\mu$ is the material parameter.

When $\xi = 0$, corresponding to $\tau = 0$, we have

$$(1+K)f_{\eta\eta\eta} + 2\eta f_{\eta\eta} + Kg_\eta = 0, \tag{9}$$

$$\left(1+\frac{K}{2}\right)g_{\eta\eta} + 2g + 2\eta g_\eta = 0, \tag{10}$$

and when $\xi = 1$, corresponding to $\tau \to \infty$, we have

$$(1+K)f_{\eta\eta\eta} + Kg_\eta + 1 + ff_{\eta\eta} - f_\eta^2 = 0, \tag{11}$$

$$(1+\frac{K}{2})g_{\eta\eta} + fg_\eta - gf_\eta - K\left(2g + f_{\eta\eta}\right) = 0. \tag{12}$$

Further, we notice that for $n = 1/2$ (weak concentration of microelements), it holds

$$g = -\frac{1}{2}f_{\eta\eta}, \tag{13}$$

and Eqs. (6) and (7) reduce to the following form:

$$\left(1+\frac{K}{2}\right)f_{\eta\eta\eta} + (1-\xi^2)\left[2\eta f_{\eta\eta} - 2\xi f_{\eta\xi}\right] + \xi^2\left[1 + ff_{\eta\eta} - f_\eta^2\right] = 0, \tag{14}$$

subject to the boundary conditions

$$f(0,\xi) = 0, \quad f_\eta(0,\xi) = 0, \quad f_\eta(\infty,\xi) = 1. \tag{15}$$

Accordingly, when $\xi = 0$, corresponding to $\tau = 0$, we have

$$\left(1+\frac{K}{2}\right)f_{\eta\eta\eta} + 2\eta f_{\eta\eta} = 0, \tag{16}$$

and when $\xi = 1$, corresponding to $\tau \to \infty$, we have

$$\left(1+\frac{K}{2}\right)f_{\eta\eta\eta} + 1 + ff_{\eta\eta} - f_\eta^2 = 0. \tag{17}$$

The local skin friction coefficient C_f is defined as

$$C_f = \frac{\tau_w}{\rho(ax)\sqrt{va}},$$

where τ_w is the wall skin friction given by

$$\tau_w = \left[(\mu + \kappa)\frac{\partial u}{\partial y} + \kappa N\right]_{y=0}. \tag{18}$$

Using variables (5) and the boundary conditions (8), we obtain

$$C_f = \frac{1}{\xi}[(1 + (1-n)K]\left(\frac{\partial^2 f}{\partial \eta^2}\right)_{\eta=0}. \tag{19}$$

3 Homotopy analysis solution

To enhance the convergence of our approximations, we introduce the transformation

$$\zeta = \lambda\eta, \tag{20}$$

where $\lambda > 0$ is a spatial-scale parameter. Using (20), Eqs. (6) and (7) become

$$(1+K)\lambda^3 f_{\zeta\zeta\zeta} + (1-\xi^2)\lambda[2\zeta f_{\zeta\zeta} - 2\xi f_{\zeta\xi}] + K\lambda g_\zeta + \xi^2\left[1 + \lambda^2 f f_{\zeta\zeta} - \lambda^2 f_\zeta^2\right] = 0, \tag{21}$$

$$(1+\frac{K}{2})\lambda^2 g_{\zeta\zeta} + (1-\xi^2)[2g + 2\zeta g_\zeta - 2\xi g_\xi] + \xi^2\left[\lambda f g_\zeta - \lambda g f_\zeta - K\left(2g + \lambda^2 f_{\zeta\zeta}\right)\right] = 0, \tag{22}$$

subject to the boundary conditions

$$f(0,\xi) = f_\zeta(0,\xi) = 0, \quad g(0,\xi) = -n\lambda^2 f_{\zeta\zeta}(0,\xi), \quad f_\zeta(\infty,\xi) = \lambda, \quad g(\infty,\xi) = 0. \tag{23}$$

From the boundary conditions (23), it is obvious that $f(\zeta,\xi)$ and $g(\zeta,\xi)$ can be expressed by a set of base functions

$$\{\xi^{2k}\,\zeta^m\,\exp(-n\zeta)|\,k \geq 0,\, n \geq 0,\, m \geq 0\} \tag{24}$$

in the form

$$f(\zeta,\xi) = \sum_{k=0}^{+\infty}\sum_{m=0}^{+\infty}\sum_{n=1}^{+\infty} a_{m,n}^k \xi^{2k}\zeta^m \exp(-n\zeta), \tag{25}$$

$$g(\zeta,\xi) = \sum_{k=0}^{+\infty}\sum_{m=0}^{+\infty}\sum_{n=1}^{+\infty} b_{m,n}^k \xi^{2k}\zeta^m \exp(-n\zeta), \tag{26}$$

where $a_{m,n}^k$ and $b_{m,n}^k$ are coefficients. These provide us with *Solution Expressions* for $f(\zeta,\xi)$ and $g(\zeta,\xi)$, respectively. Based on the boundary conditions (23) and *Solution Expressions* denoted by (25) and (26), it is straightforward to choose

$$f_0(\zeta,\xi) = \lambda[\exp(-\zeta) + \zeta - 1], \quad g_0(\zeta,\xi) = 0, \tag{27}$$

as the initial approximations of $f(\zeta,\xi)$ and $g(\zeta,\xi)$, and besides to choose

$$\mathscr{L}_f[F(\xi,\zeta;q)] = \frac{\partial^3 F}{\partial\zeta^3} - \frac{\partial F}{\partial\zeta}, \tag{28}$$

$$\mathscr{L}_g[G(\xi,\zeta;q)] = \frac{\partial^2 G}{\partial\zeta^2} - G, \tag{29}$$

as the auxiliary linear operators, which have the following properties:

$$\mathscr{L}_f[C_1\exp(-\zeta)+C_2\exp(\zeta)+C_3]=0, \tag{30}$$

$$\mathscr{L}_g[C_4\exp(-\zeta)+C_5\exp(\zeta)]=0, \tag{31}$$

respectively, where C_1, C_2, C_3, C_4 and C_5 are constants. From Eqs. (21) and (22), we are led to define the nonlinear operators

$$\begin{aligned}\mathscr{N}_f[F(\zeta,\xi;q)] &= (1+K)\lambda^3\frac{\partial^3 F}{\partial\zeta^3}+(1-\xi^2)\lambda\left[2\zeta\frac{\partial^2 F}{\partial\zeta^2}-2\xi\frac{\partial^2 F}{\partial\zeta\partial\xi}\right]\\ &\quad +K\lambda\frac{\partial G}{\partial\zeta}+\xi^2\left[1+\lambda^2 F\frac{\partial^2 F}{\partial\zeta^2}-\lambda^2\left(\frac{\partial F}{\partial\zeta}\right)^2\right],\end{aligned} \tag{32}$$

$$\begin{aligned}\mathscr{N}_g[G(\zeta,\xi;q)] &= (1+\frac{K}{2})\lambda^2\frac{\partial^2 G}{\partial\zeta^2}+(1-\xi^2)\left[2G+2\zeta\frac{\partial G}{\partial\zeta}-2\xi\frac{\partial G}{\partial\xi}\right]\\ &\quad +\xi^2\left[\lambda F\frac{\partial G}{\partial\zeta}-\lambda G\frac{\partial F}{\partial\zeta}-K\left(2G+\lambda^2\frac{\partial^2 F}{\partial\zeta^2}\right)\right].\end{aligned} \tag{33}$$

Then, let $\hbar_f$ and $\hbar_g$ denote the auxiliary parameters. We construct the zeroth-order deformation equations

$$(1-q)\mathscr{L}_f[F(\zeta,\xi;q)-f_0(\zeta,\xi)]=q\,\hbar_f\,\mathscr{N}_f[F(\zeta,\xi;q),G(\zeta,\xi;q)], \tag{34}$$

$$(1-q)\mathscr{L}_g[G(\zeta,\xi;q)-g_0(\zeta,\xi)]=q\,\hbar_g\,\mathscr{N}_g[F(\zeta,\xi;q),G(\zeta,\xi;q)], \tag{35}$$

subject to the boundary conditions

$$\begin{aligned}&F(0,\xi;q)=\left.\frac{\partial F(\zeta,\xi;q)}{\partial\zeta}\right|_{\zeta=0}=0,\quad G(0,\xi;q)=n\lambda^2\left.\frac{\partial^2 F(\zeta,\xi;q)}{\partial\zeta^2}\right|_{\zeta=0},\\ &G(\infty,\xi;q)=0,\quad \left.\frac{\partial F(\zeta,\xi;q)}{\partial\zeta}\right|_{\zeta=+\infty}=\lambda,\end{aligned} \tag{36}$$

where $q\in[0,1]$ is an embedding parameter. Obviously, when $q=0$ and $q=1$, the above zeroth-order deformation equations (34) and (35) have the solutions

$$F(\zeta,\xi;0)=f_0(\zeta,\xi),\quad G(\zeta,\xi;0)=g_0(\zeta,\xi), \tag{37}$$

and

$$F(\zeta,\xi;1)=f(\zeta,\xi),\quad G(\zeta,\xi;1)=g(\zeta,\xi), \tag{38}$$

respectively. Expanding $F(\zeta,\xi;q)$ and $G(\zeta,\xi;q)$ in Taylor's series with respect to q, we have

$$F(\zeta,\xi;q)=F(\zeta,\xi,0)+\sum_{m=1}^{+\infty}f_m(\zeta,\xi)q^m, \tag{39}$$

$$G(\zeta,\xi;q)=G(\zeta,\xi,0)+\sum_{m=1}^{+\infty}g_m(\zeta,\xi)q^m, \tag{40}$$

where

$$f_m(\zeta,\xi)=\frac{1}{m!}\left.\frac{\partial^m F(\zeta,\xi;q)}{\partial q^m}\right|_{q=0},\quad g_m(\zeta,\xi)=\frac{1}{m!}\left.\frac{\partial^m G(\zeta,\xi;q)}{\partial q^m}\right|_{q=0}, \tag{41}$$

respectively. Note that Eqs. (34) and (35) contain two auxiliary parameters $\hbar_f$ and $\hbar_g$. Assuming that all of them are correctly chosen so that the above series are convergent at $q = 1$, we have, using Eq. (37), the solution series

$$f(\zeta,\xi) = f_0(\zeta,\xi) + \sum_{m=1}^{+\infty} f_m(\zeta,\xi), \tag{42}$$

$$g(\zeta,\xi) = g_0(\zeta,\xi) + \sum_{m=1}^{+\infty} g_m(\zeta,\xi). \tag{43}$$

Define vectors

$$\vec{f}_m = \{f_0, f_1, f_2, \ldots, f_m\}, \quad \vec{g}_m = \{g_0, g_1, g_2, \ldots, g_m\}. \tag{44}$$

Differentiating the zeroth-order deformation equations (34) and (35) m times with respect to q, then setting $q = 0$, and finally dividing them by $m!$, we obtain the mth-order deformation equations

$$\mathscr{L}_f[f_m(\zeta,\xi) - \chi_m f_{m-1}(\zeta,\xi)] = \hbar_f R_m^f(\vec{f}_{m-1}, \vec{g}_{m-1}), \tag{45}$$

$$\mathscr{L}_g[g_m(\zeta,\xi) - \chi_m g_{m-1}(\zeta,\xi)] = \hbar_g R_m^g(\vec{f}_{m-1}, \vec{g}_{m-1}), \tag{46}$$

subject to the boundary conditions

$$\begin{aligned} &g_m(0,\xi) = n\lambda^2 \frac{\partial^2 f_m(\zeta,\xi)}{\partial\zeta^2}\bigg|_{\zeta=0}, \quad f_m(0,\xi) = \frac{\partial f_m(\zeta,\xi)}{\partial\zeta}\bigg|_{\zeta=0} = 0, \\ &g_m(\infty,\xi) = 0, \quad \frac{\partial f_m(\zeta,\xi)}{\partial\zeta}\bigg|_{\zeta=\infty} = 0, \end{aligned} \tag{47}$$

where

$$\begin{aligned} R_m^f(\vec{f}_{m-1}, \vec{g}_{m-1}) = {} & (1+K)\lambda^3 \frac{\partial^3 f_{m-1}}{\partial\zeta^3} + (1-\xi^2)\lambda\left[2\zeta\frac{\partial^2 f_{m-1}}{\partial\zeta^2} - 2\xi\frac{\partial^2 f_{m-1}}{\partial\zeta\partial\xi}\right] \\ & + K\lambda\frac{\partial g_{m-1}}{\partial\zeta} + \xi^2\left[1 - \chi_m + \lambda^2\sum_{i=0}^{m-1} f_i\frac{\partial^2 f_{m-1-i}}{\partial\zeta^2} - \lambda^2\sum_{i=0}^{m-1}\frac{\partial f_i}{\partial\zeta}\frac{\partial f_{m-1-i}}{\partial\zeta}\right] \end{aligned} \tag{48}$$

and

$$\begin{aligned} R_m^g(\vec{f}_{m-1}, \vec{g}_{m-1}) = {} & \left(1 + \frac{K}{2}\right)\lambda^2\frac{\partial^2 g_{m-1}}{\partial\zeta^2} + (1-\xi^2)\left[2g_{m-1} + 2\zeta\frac{\partial g_{m-1}}{\partial\zeta} - 2\xi\frac{\partial g_{m-1}}{\partial\xi}\right] \\ & + \xi^2\left[\lambda\sum_{i=0}^{m-1} f_i\frac{\partial g_{m-1-i}}{\partial\zeta} - \lambda\sum_{i=0}^{m-1} g_i\frac{\partial f_{m-1-i}}{\partial\zeta} - K\left(2g_{m-1} + \lambda^2\frac{\partial^2 f_{m-1}}{\partial\zeta^2}\right)\right], \end{aligned} \tag{49}$$

under the definition

$$\chi_m = \begin{cases} 0, & m = 1, \\ 1, & m > 1. \end{cases} \tag{50}$$

Let $f_m^*(\zeta,\xi)$ and $g_m^*(\zeta,\xi)$ denote the special solutions of Eqs. (45) and (46). From Eqs. (30) and (31), their general solutions read

$$f_m(\zeta,\xi) = f_m^*(\zeta,\xi) + C_1\exp(-\zeta) + C_2\exp(\zeta) + C_3, \tag{51}$$

$$g_m(\zeta,\xi) = g_m^*(\zeta,\xi) + C_4\exp(-\zeta) + C_5\exp(\zeta), \tag{52}$$

where the integral constants C_1, C_2, C_3, C_4, and C_5 are determined by the boundary conditions (47).

In this way, it is easy to solve the linear equations (45) and (46), one after the other in the order $m = 1, 2, 3$.

When $n = 1/2$, substituting (13) into Eqs. (11), then using (20), it holds

$$\left(1+\frac{K}{2}\right)\lambda^3 f_{\zeta\zeta\zeta} + (1-\xi^2)\lambda[2\zeta f_{\zeta\zeta} - 2\xi f_{\zeta\xi}] + \xi^2\left[1 + \lambda^2 f f_{\zeta\zeta} - \lambda^2 f_\zeta^2\right] = 0, \tag{53}$$

subject to the boundary conditions

$$f(0,\xi) = 0, \quad f_\zeta(0,\xi) = 0, \quad f_\zeta(\infty,\xi) = \lambda. \tag{54}$$

Similarly, by using the above-mentioned method, we can obtain the series solutions for the case $n = 1/2$.

4 Result analysis

Liao [17] proved that, as long as a solution series given by the homotopy analysis method converges, it must be one of solutions. Note that the solution series (42) and (43) contain three unknown parameters, the spatial-scale parameter λ, the auxiliary parameters $\hbar_f$ and $\hbar_g$. These parameters can be determined in the way described below. The residual error of the initial guess $f_0(\xi,\zeta)$ can be expressed by

$$E_0(\lambda) = \int_0^1 \int_0^\infty (R_1^f[\vec{f}_0, \vec{g}_0])^2 d\xi d\zeta, \tag{55}$$

which is only dependent on λ. Let

$$\frac{dE_0}{d\lambda} = 0, \tag{56}$$

we can get the best value of λ by solving the above equation. Then we can choose properly the values of $\hbar_f$ and $\hbar_g$ by plotting the $\hbar$-curves to ensure that the solution series (42) and (43) converge, as suggested by Liao [17]. The values of $\hbar_f$, $\hbar_g$ and λ used in our calculation are listed in Table 1.

When $\xi = 0$, corresponding to the initial state, and when $\xi = 1$, corresponding to the steady state, our series solutions agree well with numerical ones in the whole region $0 \le \eta < +\infty$, as shown in Figs. 2–4. Note that the numerical results are obtained by using the finite difference method based on the homotopy analysis method [34] and Newton-Raphson technique. The initial guesses of the numerical solutions are given by $f_0(\eta) = \eta - 1 + \exp(-\eta)$ and $g_0(\eta) = 0$. To satisfy the boundary conditions at infinity, an integration distance $\eta_\infty = 40$, which is discretized into 10000 intervals, is found to be adequate. The iterative integration procedure is repeated until the errors for each discretized Eqs. (11) and (12) are less than 5×10^{-6}. Similarly, in the whole region $\xi \in [0,1]$, the solution series (42) and (43) are convergent when we set the proper values of $\hbar_f$ and $\hbar_g$, as shown in Figs. 5 and 6. In fact, we find that our solution series (42) and (43) are convergent for all $\xi \in [0,1]$. Thus, by means of homotopy analysis method, we obtain accurate series solutions uniformly valid for all $\xi \in [0,1]$ in the whole region $0 \le \eta < +\infty$.

The dimensionless velocity profiles $f_\eta(\eta,\xi)$ as functions of τ for some values of the parameter K when $n = 0$ (strong concentration of microelements) and when $n = 1/2$ (weak concentration

Table 1. The values of parameters used in our calculation

λ	$\hbar_f$	$\hbar_g$	K	n
–	–	–	0	0
3	$-1/40$	$-1/30$	1	0
3	$-1/50$	$-1/25$	3	0
5/2	$-1/70$	$-1/30$	5	0
2	$-1/60$	$-1/40$	10	0
4	$-1/60$	–	0	0.5
3	$-1/40$	–	1	0.5
3	$-1/50$	–	3	0.5
5/2	$-1/40$	–	5	0.5
2	$-1/40$	–	10	0.5

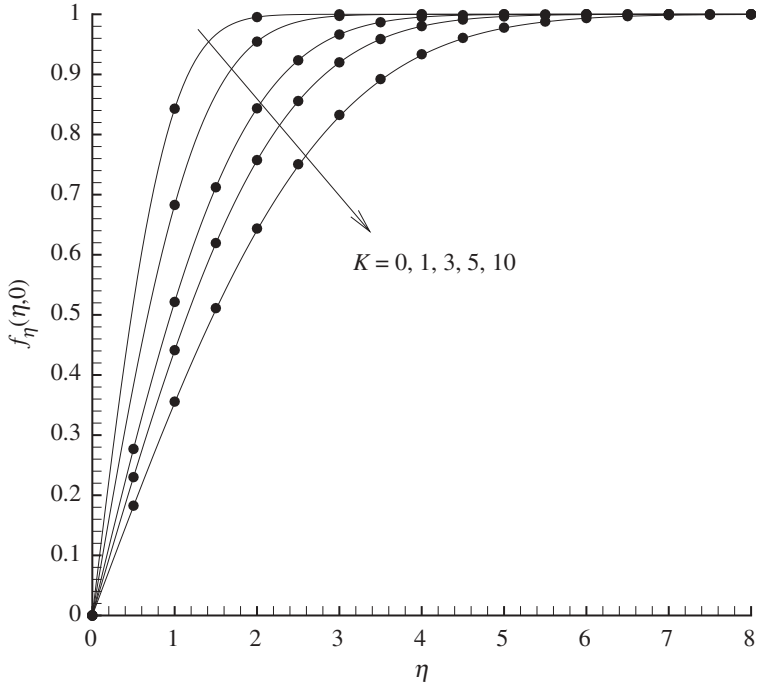

Fig. 2. The comparison of $f_\eta(\eta, 0)$ of the numerical results with the HAM approximations for different values of K when $n = 0$. Symbol: Numerical results; solid line: 25th-order approximations

of microelements) are shown in Fig. 7 as τ increases from $\tau = 0$ (initial unsteady flow) to $\tau \to \infty$ (steady-state flow). The dimensionless microrotation profiles $g(\eta, \xi)$ as functions of τ for some values of the parameter K when $n = 0$ (strong concentration of microelements) are shown in Fig. 8 as τ increases from $\tau = 0$ (initial unsteady flow) to $\tau \to \infty$ (steady-state flow). The graphs for $\tau = 2$ and $\tau \to \infty$ are almost indistinguishable. The variable $y\sqrt{a/\nu} = \eta\xi$ in place of η has been used. We can see that these profiles develop rapidly from rest as τ increases from zero to ∞. However, it is important to notice that the transition from the unsteady initial flow up to the steady-state flow is completely smooth for all values of K and τ. For the same value of the parameter K, the thickness of the microrotation boundary layer is larger than the thickness of the velocity boundary layer. But for the same values of K, the velocity profiles are higher for

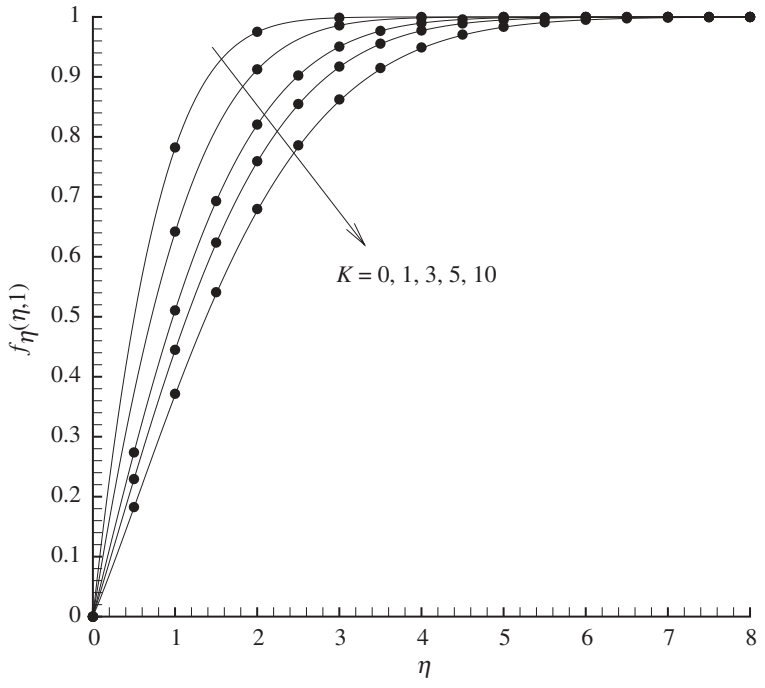

Fig. 3. The comparison of $f_\eta(\eta, 1)$ of the numerical results with the HAM approximations for different values of K when $n = 0$. Symbol: Numerical results; solid line: 25th-order approximations

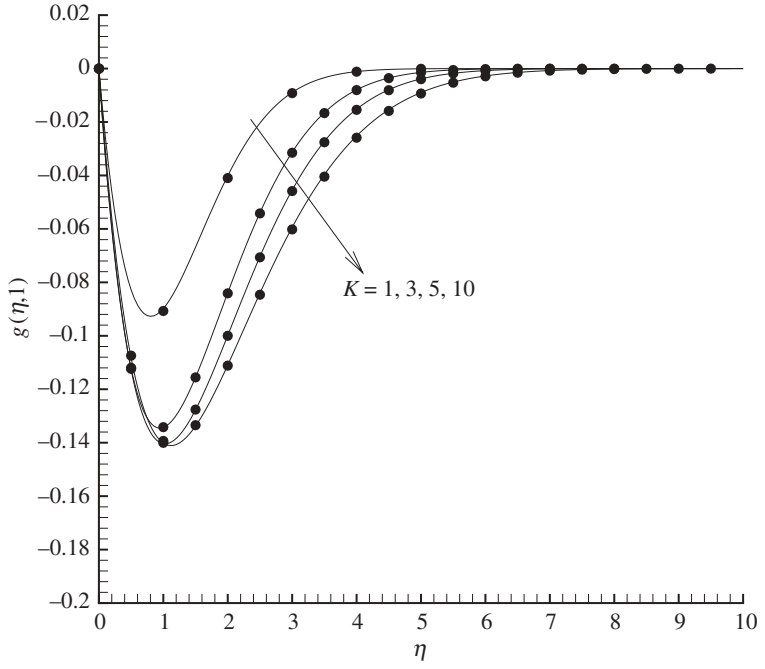

Fig. 4. The comparison of $g(\eta, 1)$ of the numerical results with the HAM approximations for different values of K when $n = 0$. Symbol: Numerical results; solid line: 25th-order approximations

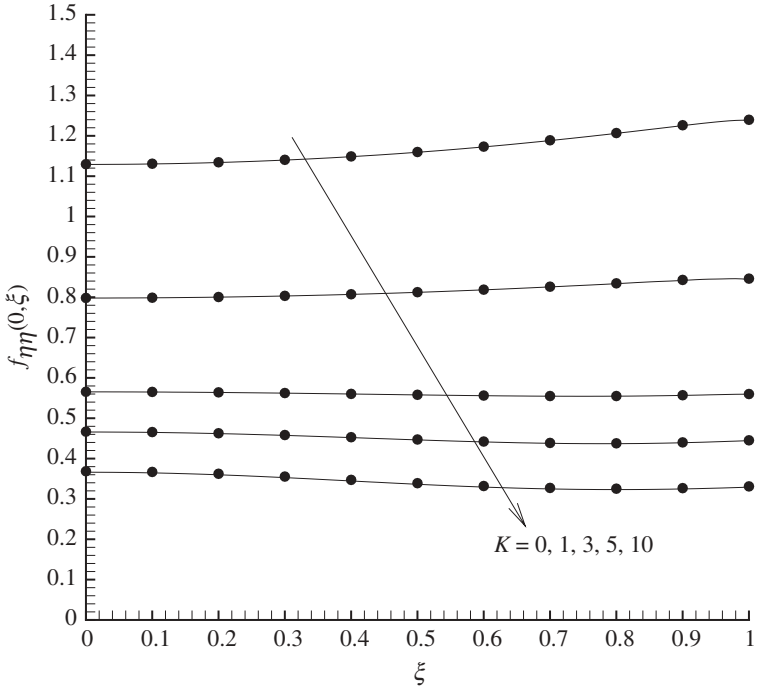

Fig. 5. The HAM approximations of $f_{\eta\eta}(0,\xi)$ for $0 \leq \xi \leq 1$ when $n = 0$. Solid line: 20th-order approximations; Symbols: 25th-order approximations

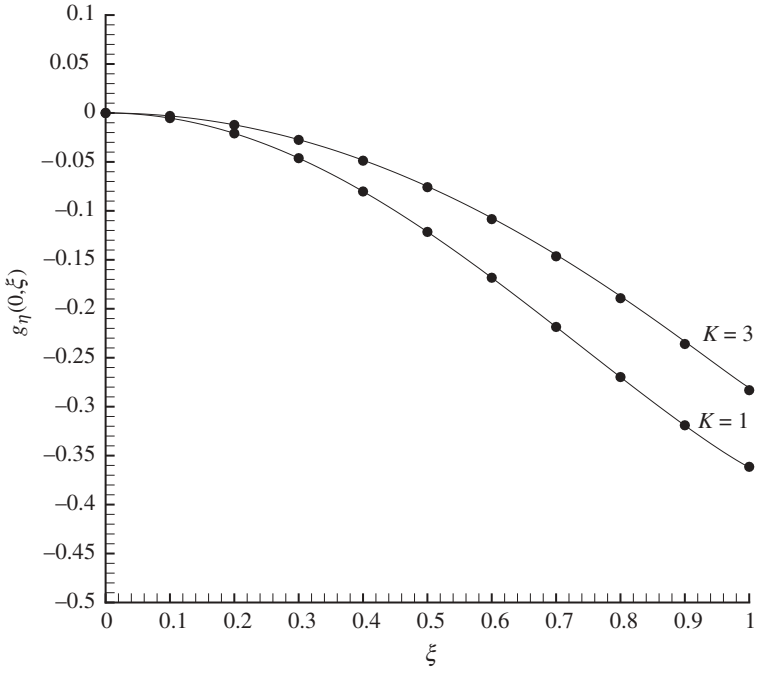

Fig. 6. The HAM approximations of $g_{\eta}(0,\xi)$ for $0 \leq \xi \leq 1$ when $n = 0$. Solid line: 20th-order approximations; Symbols: 25th-order approximations

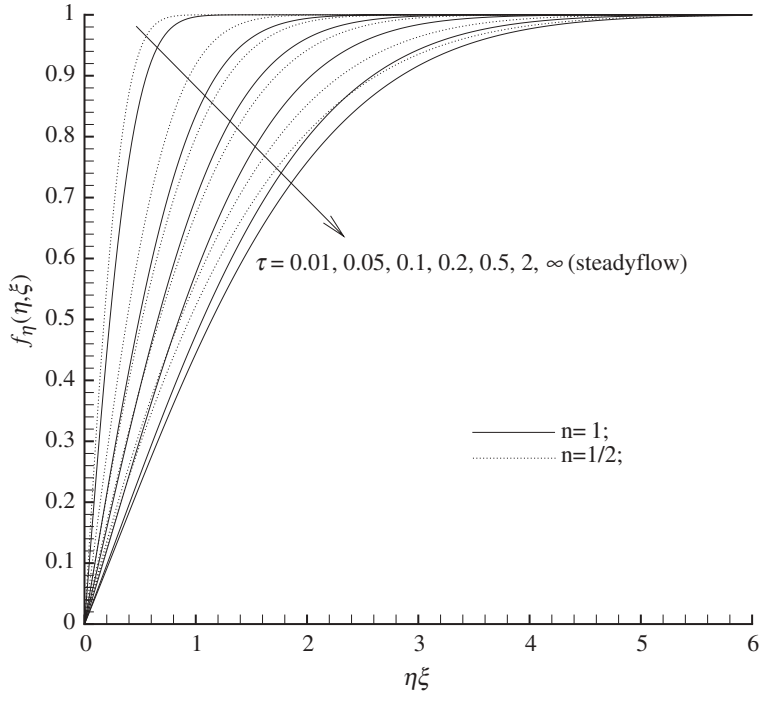

Fig. 7. The velocity profiles for the forward stagnation point when $K = 1$

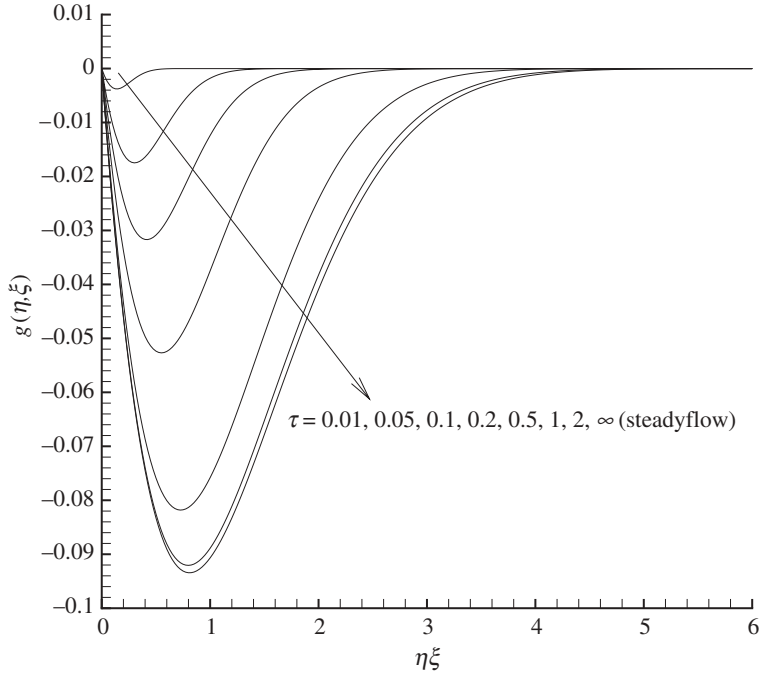

Fig. 8. The microrotation profiles for the forward stagnation point when $K = 1$ and $n = 0$

$n = 1/2$ than for $n = 0$, as shown in Fig. 7. We also notice from Fig. 8 that the microrotation profile $g(\eta, \xi)$ reaches a minimum at a finite distance from the wall. It is also clear from this figure that as the local minimum moves away from the wall the corresponding boundary layer thickness increases. Since the present problem of the micropolar boundary-layer flow has steady solutions with positive skin friction, separation will not occur and unsteady flows will approach the steady-state flow as a limit of $\tau \to \infty$. Although not shown here, it was found, as expected, that the effect of K is such that the velocity boundary layer thickness decreases slightly with an increase in K.

The local skin friction coefficient C_f versus τ for some values of the parameter K when $n = 0$ (strong concentration of microelements) is shown in Fig. 9, when $n = 1/2$ (weak concentration of microelements) is shown in Fig. 10. It is seen that the coefficient of skin friction decreases continuously for each value of the parameter K considered as time τ elapses and is asymptotic to that of steady-state flow as a limit of $\tau \to \infty$. Therefore the transition from the initial unsteady flow to the final steady-state flow is smooth, i.e., without any singularity. Micropolar fluid flow ($K > 0$) generates, largely because of the vortex viscosity (cf. $K = \kappa/\mu$), higher skin friction coefficients, as can be seen from Figs. 9 and 10. A similar trend was also found by Lok et al. [11].

5 Conclusions

In this paper, we apply the homotopy analysis method to study the unsteady boundary-layer flow of a micropolar fluid near the forward stagnation point of an infinite plane wall and obtain

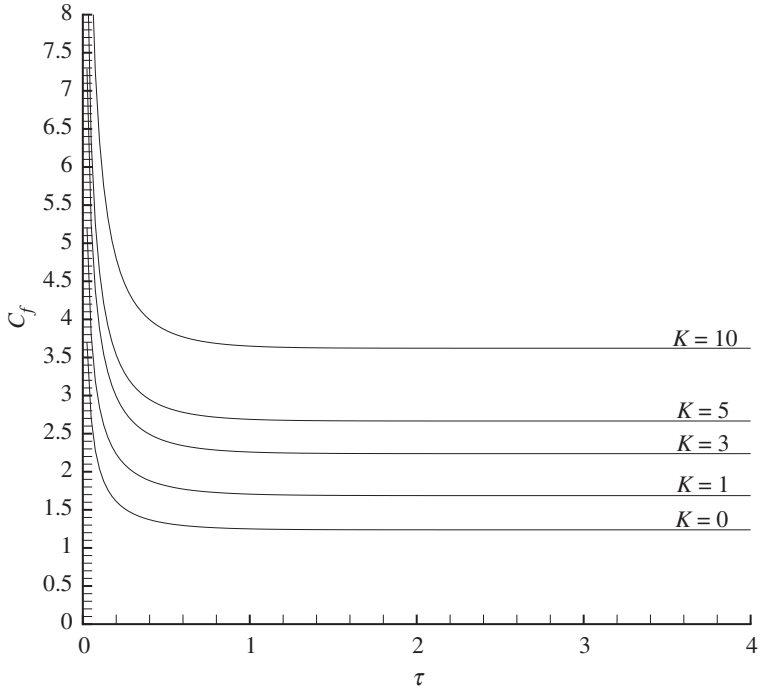

Fig. 9. The variation of the skin friction coefficient as a function of τ for different parameters K when $n = 0$

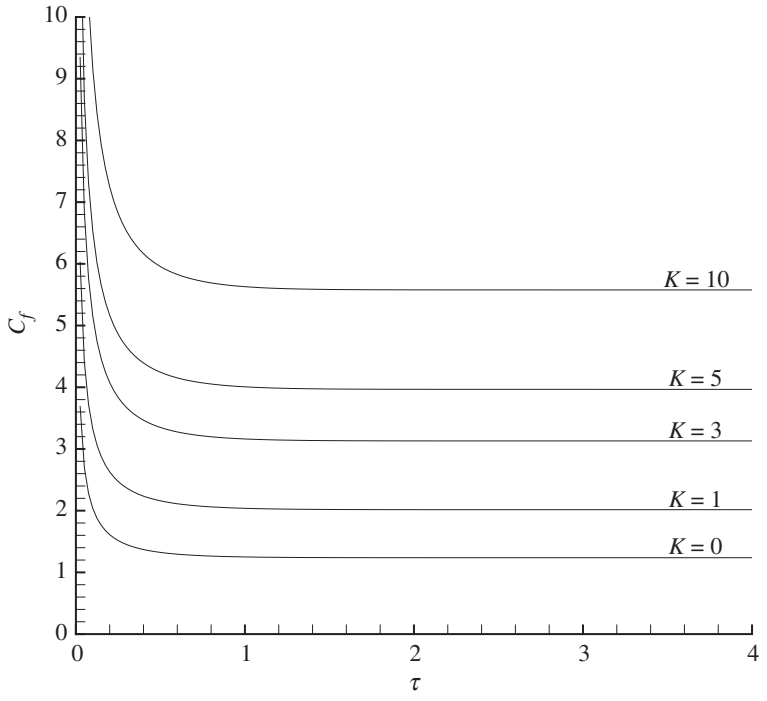

Fig. 10. The variation of the skin friction coefficient as a function of τ for different parameters K when $n = 0.5$

the uniformly valid series solutions of this problem. Different from previous series solutions, our solutions are valid for all time $0 \leq \tau < \infty$ and in the whole region $0 \leq \eta < \infty$. The effects of the material parameter K on the velocity and microrotation for $n = 0$ and $n = 0.5$ are also discussed. To the best of our knowledge, such kinds of series solutions have never been reported. The proposed analytic approach has general meaning and thus may be applied in a similar way to other unsteady boundary-layer flows to get accurate series solutions valid for all time.

Acknowledgements

Thanks to anonymous reviewers for their valuable suggestions.

References

[1] Hiemenz, K.: Die Grenzschicht an einem in den gleichförmigen Flüssigkeitsstrom eingetauchten geraden Kreiszylinder. Dinglers Polym. J. **326**, 321–410 (1911).
[2] Homann, F.: Der Einfluß großer Zähigkeit bei der Strömung um den Zylinder und um die Kugel. Z. Angew. Math. Mech. **16**, 153–164 (1936).
[3] Wang, C. Y.: Axisymmetric stagnation flow on a cylinder. Q. Appl. Math. **32**, 207–213 (1974).
[4] Gorla, R. S. R.: Boundary-layer flow of a micropolar fluid in the vicinity of an axisymmetric stagnation point on a cylinder. Int. J. Engng. Sci. **28**, 145–152 (1990).
[5] Proudman, I., Johnson, K.: Boundary-layer growth near a rear stagnation point. J. Fluid. Mech. **12**, 161–168 (1962).

[6] Robins, A. J., Howarth, J. A.: Boundary layer development of a two-dimensional rear stagnation point. J. Fluid. Mech. **56**, 161–172 (1972).
[7] Howarth, J. A.: A note on boundary-layer growth at an axisymmetric rear stagnation point. J. Fluid. Mech. **59**, 769–773 (1973).
[8] Howarth, J. A.: Boundary-layer growth at a three-dimensional rear stagnation point. J. Fluid. Mech. **67**, 289–297 (1975).
[9] Katagiri, M.: Unsteady magnetohydrodynamic flow at the forward stagnation point. J. Phys. Soc. Japan **27**, 1662–1668 (1969).
[10] Burdé, G. I.: The construction of special explicit solutions of the boundary-layer equations of unsteady flows. Quart. J. Mech. Appl. Math. **48**, 611–633 (1995).
[11] Lok, Y. Y., Phang, P., Amin, N., Pop, I.: Unsteady boundary layer flow of a micropolar fluid near the forward stagnation point of a plane surface. Int. J. Engng. Sci. **41**, 173–186 (2003).
[12] Eringen, A. C.: Theory of micropolar fluids. J. Math. Mech. **16**, 1–18 (1966).
[13] Eringen, A. C.: Theory of thermomicropolar fluids. J. Math. Anal. Appl. **38**, 480–496 (1972).
[14] Ariman, T., Turk, M. A., Sylvester, N. D.: Microcontinuum fluid mechanics-a review. Int. J. Engng. Sci. **11**, 905–930 (1973).
[15] Lukaszewicz, G.: Micropolar fluids: theory and application. Basel: Birkhäuser 1998.
[16] Eringen, A. C.: Microcontinuum field theories. II: fluent media. New York: Springer 2001.
[17] Liao, S. J.: Beyond perturbation: introduction to homotopy analysis method. Boca Raton: Chapman & Hall/CRC Press 2003.
[18] Nayfeh, A. H.: Perturbation methods. New York: Wiley 2000.
[19] Lyapunov, A. M.: General problem on stability of motion. London: Taylor & Francis 1992 (English translation).
[20] Karmishin, A. V., Zhukov, A. T., Kolosov, V. G.: Methods of dynamics calculation and testing for thin-walled structures. Moscow: Mashinostroyenie 1990 (in Russian).
[21] Adomian, G.: Nonlinear stochastic differential equations. J. Math. Anal. Appl. **55**, 441–452 (1976).
[22] Liao, S. J., Campo, A.: Analytic solutions of the temperature distribution in Blasius viscous flow problems. J. Fluid Mech. **453**, 411–425 (2002).
[23] Liao, S. J.: On the analytic solution of magnetohydrodynamic flows of non-Newtonian fluids over a stretching sheet. J. Fluid Mech. **488**, 189–212 (2003).
[24] Liao, S. J., Pop, I.: Explicit analytic solution for similarity boundary layer equations. Int. J. Heat Mass Transf. **47**, 75–85 (2004).
[25] Xu, H.: An explicit analytic solution for free convection about a vertical flat plate embedded in a porous medium by means of homotopy analysis method. Appl. Math. Comput. **158**, 433–443 (2004).
[26] Riley, N.: Unsteady laminar boundary layers. SIAM Review **17**, 274–297 (1975).
[27] Rees, D. A. S., Bassom, A. P.: The Blasius boundary layer flow of a micropolar fluid. Int. J. Engng. Sci. **34**, 113–124 (1996).
[28] Rees, D. A. S., Pop, I.: Free convection boundary-layer flow of a micropolar fluid from a vertical flat plate. IMA J. Appl. Math. **61**, 179–197 (1998).
[29] Nazar, N., Amin, N., Pop, I.: Unsteady boundary layer flow due to a stretching surface in a rotating fluid. Mech. Res. Commun. **31**, 121–128 (2004).
[30] Jena, S. K., Mathur, M. N.: Similarity solutions for laminar free convection flow of a thermomicropolar fluid past a nonisothermal flat plate. Int. J. Engng. Sci. **19**, 1431–1439 (1981).
[31] Guram, G. S., Smith, C.: Stagnation flows of micropolar fluids with strong and weak interactions. Comput. Math. Appl. **6**, 213–233 (1980).
[32] Ahmadi, G.: Self-similar solution of incompressible micropolar boundary-layer flow over a semi-infinite flat plate. Int. J. Engng. Sci. **14**, 639–646 (1976).
[33] Peddieson, J.: An application of the micropolar fluid model to the calculation of turbulent shear flow. Int. J. Engng. Sci. **10**, 23–32 (1972).
[34] Liao, S. J.: Numerically solving non-linear problems by the homotopy analysis method. Comput. Mech. **20**, 530–540 (1997).

Authors' addresses: H. Xu and S. J. Liao, School of Naval Architecture, Ocean and Civil Engineering, Shanghai Jiao Tong University, Shanghai 200030, P. R. China (E-mail: henry629@sjtu.edu.cn); I. Pop, Faculty of Mathematics, University of Cluj, 3400 Cluj, CP253, Romania (E-mail: popi@math.ubbcluj.ro)